Effect of straining flow and droplet shape on vaporization rate of a liquid fuel droplet

Meha Setiya, PhD candidate
John Palmore Jr., Assistant Professor
Department of Mechanical Engineering,Virginia Tech

73rd Annual Meeting of the APS Division of Fluid Dynamics
November 22–24, 2020

Overview

1. Motivation
2. Numerical framework and setup
3. Results and discussion
4. Summary and Future Work
5. References

Motivation

- In spray combustion, the flow around the liquid fuel droplets is highly swirling. The droplet deformation is significant in such flow conditions.

- In past studies, both experimental and numerical, a detailed understanding of uniform flow around a rigid sphere have been developed [3] [4]. However, a limited work is available on non-uniform flow over a deforming sphere. The problem becomes even more complex when these spheres (droplets in spray combustion) are vaporizing.

- A recent analytical work on exact solutions of mass transport equations for **vaporizing and non-spherical droplets in stagnant flow** [6] indicated that the ellipsoidal droplets have the enhanced vaporization rate in comparison to iso-volume spherical droplet.

- In case of real liquid droplets, the change in vaporization rate can also be due to different boundary layer flow development as well as change in internal flow inside the droplet.

- Unfortunately, no detailed study has been performed to understand the interaction of inflow velocity profile, droplet shape and its vaporization rate. This motivates the current work to explore the relevant non-dimensional groups such as the Weber number and the non-dimensional strain rate and their effect on vaporization rate.

Numerical Framework and Setup

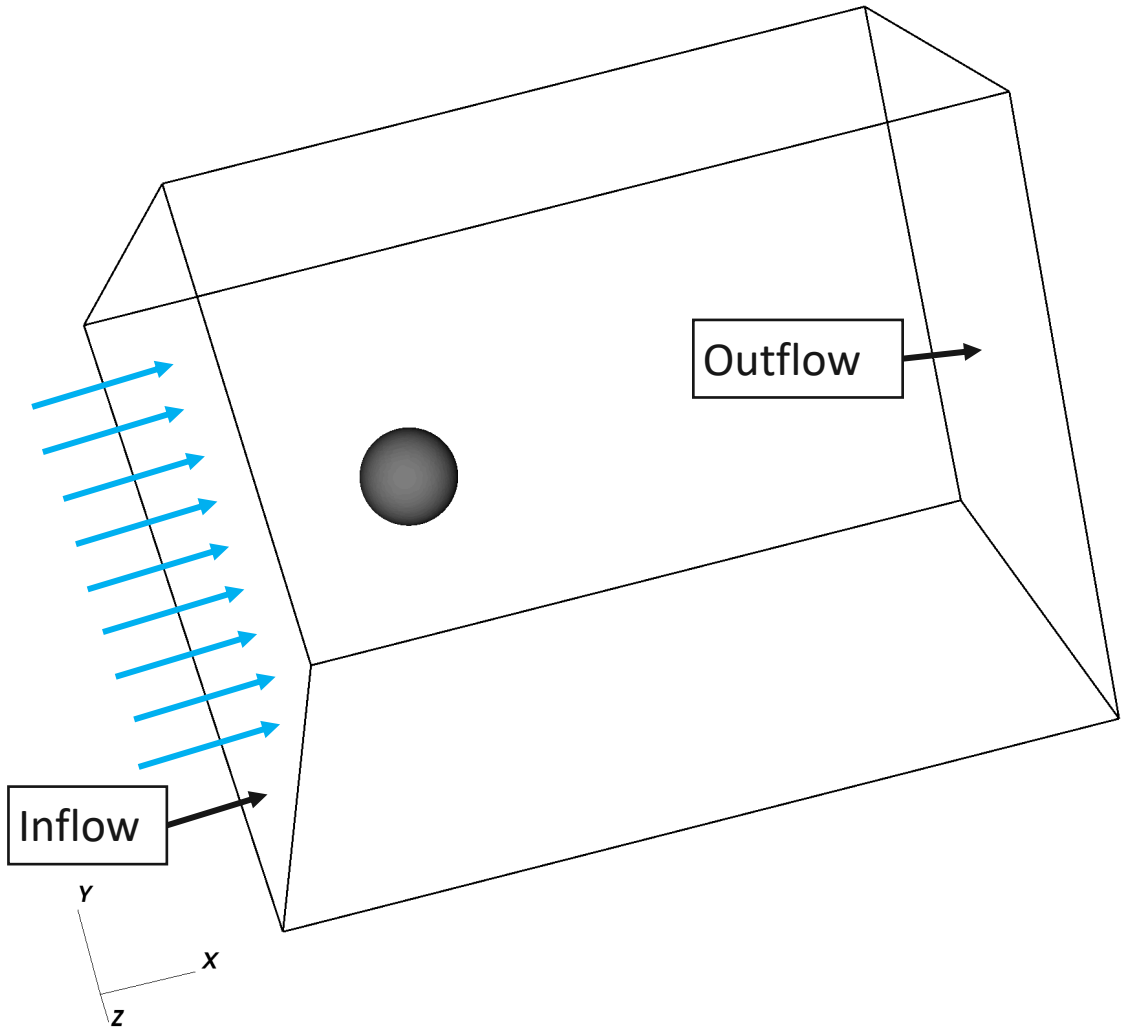

- In-house code NGA for computational studies [1].
- Interface-capturing direct numerical simulations of vaporizing multiphase flows.
- Solves the system from first principles; conservation of mass, momentum, energy and species transport.
- Fuel : single component and non-reacting with the surrounding gas.
- Diameter of the droplet d= $1\times10^{-3}\ m$
- Domain size $l_x\times l_y\times l_z = 8d \times 6d \times 6d$
- Droplet location = $(-2d, 0, 0)$
- Inflow boundary condition uses gravity update method [2].

Fuel N-decane at $T_{boil} = 447.3\ K$

Property	Units	Gas	Liquid
ρ	kg/m^3	0.789	604
μ	$kg/(m\cdot s)$	2.470×10^{-5}	1.920×10^{-5}
c_P	$J/(kg\cdot K)$	1020	2812
k	$W/(m\cdot K)$	0.037	0.094
σ	N/m	—	0.010
L_v	J/kg	—	2.763×10^5
T_{boil}	K	—	447.3

Numerical Setup : Non-uniform structured grid

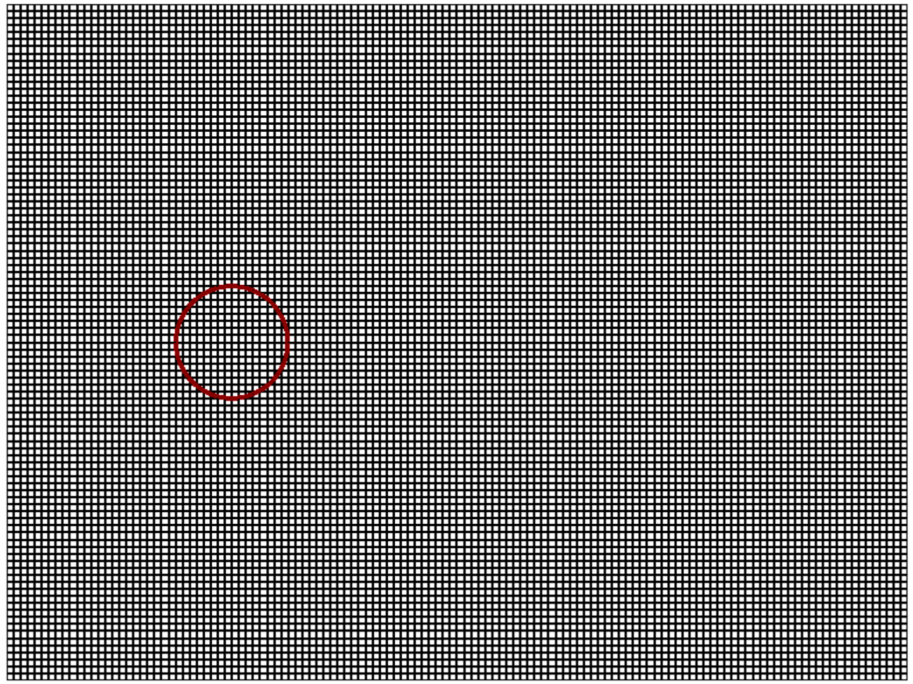

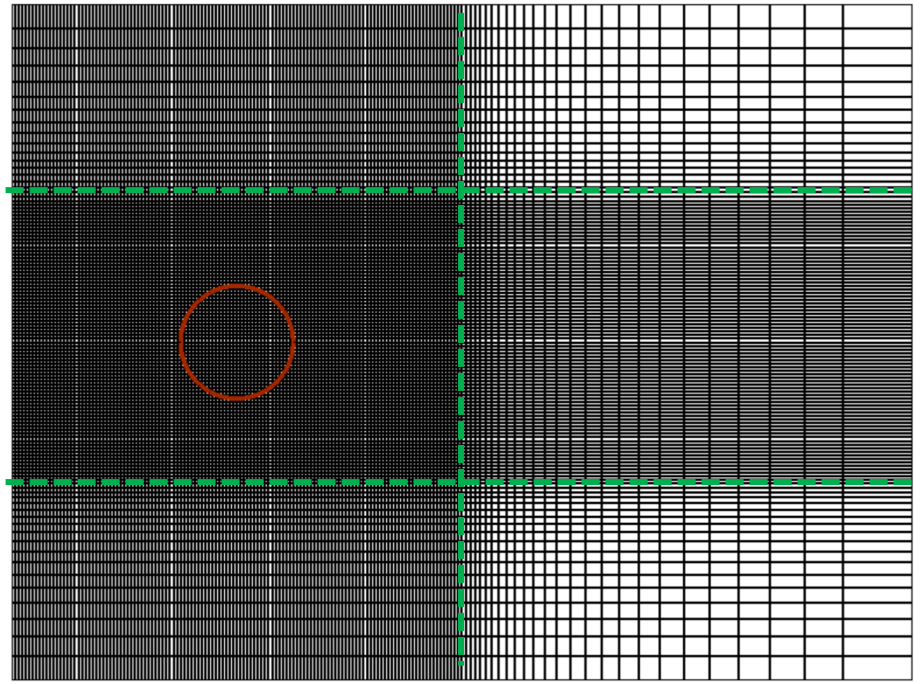

- A detailed study was performed to identify the size refined region and stretch ratio for the given flow conditions: We=12 and Re=120 uniform flow as these flow conditions would be extreme in terms of droplet deformation and flow separation.
- The % difference in vaporization flux per unit area ($\dot{m}''$) is compared for all the cases and the uniform grid. The results show that the % difference in $\ddot{m}$ w.r.t. uniform grid case is less than 5 % in case of non-uniform grid case.
- The grid convergence study is performed by changing number of cells per droplet diameter $N_d = 8, 16, 32, 64$. N_d=32 is found to be optimum grid size for this work.

Vaporizing droplets in uniform/ non-uniform flow

- Traditional gas phase heat transfer

$$Nu = Nu(Re, Pr, B)$$

- Effect of surface tension and inlet velocity profile on droplet shape

$$\frac{A_d}{A_0} = f\left(\frac{U_{in}}{sd}, Re, We\right)$$

- Combine theory -----> Gas phase heat transfer including effect of droplet shape

$$Nu = Nu\left(Re, Pr, B, \frac{A_d}{A_0}\right)$$

$$Nu = Nu\left(\underbrace{\frac{U_{in}}{sd}}_{\text{Strain velocity ratio}}, Re, We, Pr, B\right)$$

- For this work, ambient fluid is air at $P_\infty = 1\ atm$, $T_\infty = 1600\ K$.

Study 1: Total vaporization rate vs time

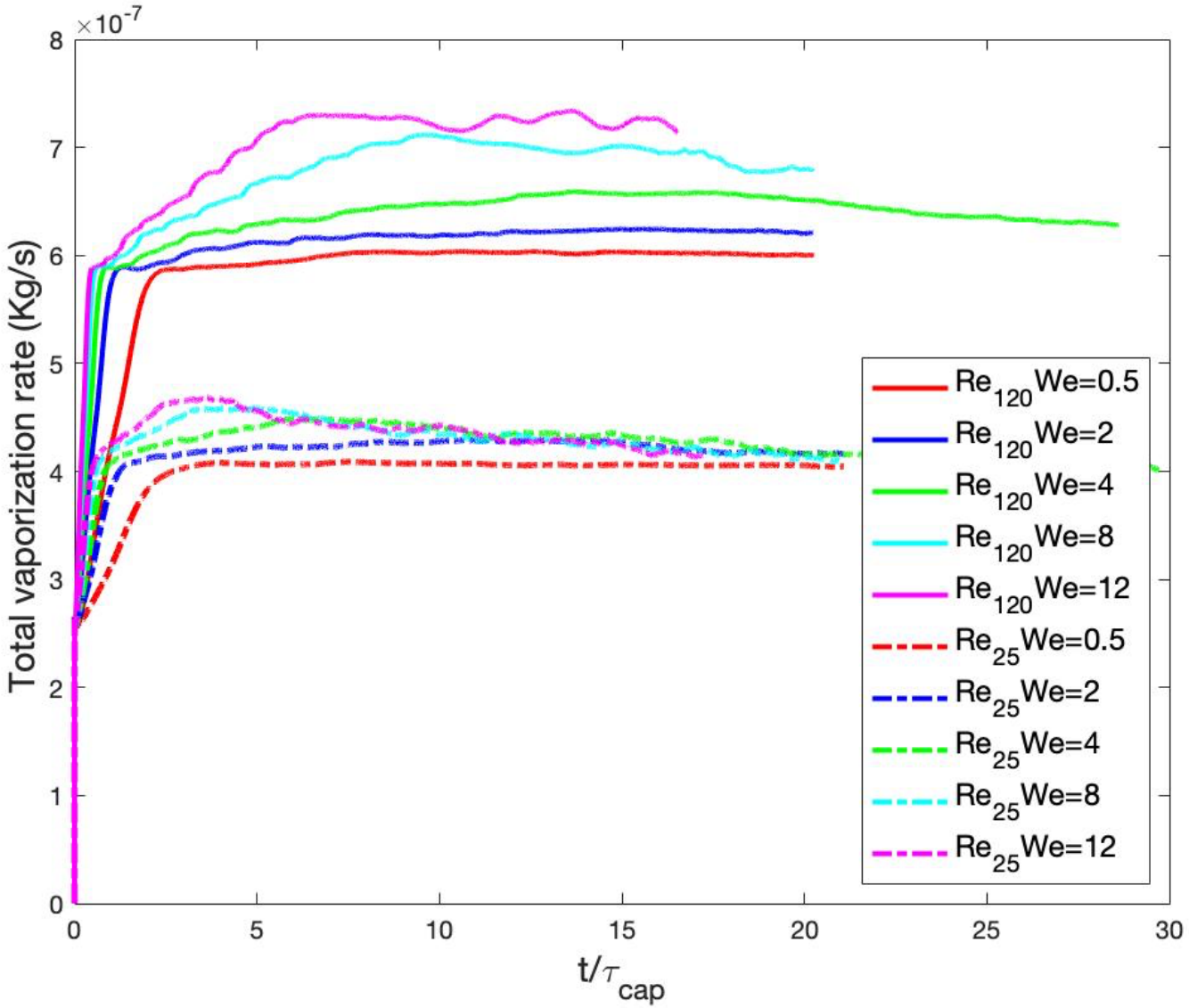

- This work covers the range of weber number from $\boldsymbol{We = 0.5\ to\ 12}$ at low and moderate Reynolds numbers.
- At low Reynold number Re=25, the difference in total vaporization rate is seen in the beginning for We=8 and 12 cases. However, at later time, the total vaporization decreases and reaches a lower steady value.
- At Re=120, significant increase in total vaporization rate is observed with change in Weber number. This difference has contribution both from vaporization flux $\dot{m}''$ and change in total surface area of the droplet.

Study 1: Normalized total surface area vs time

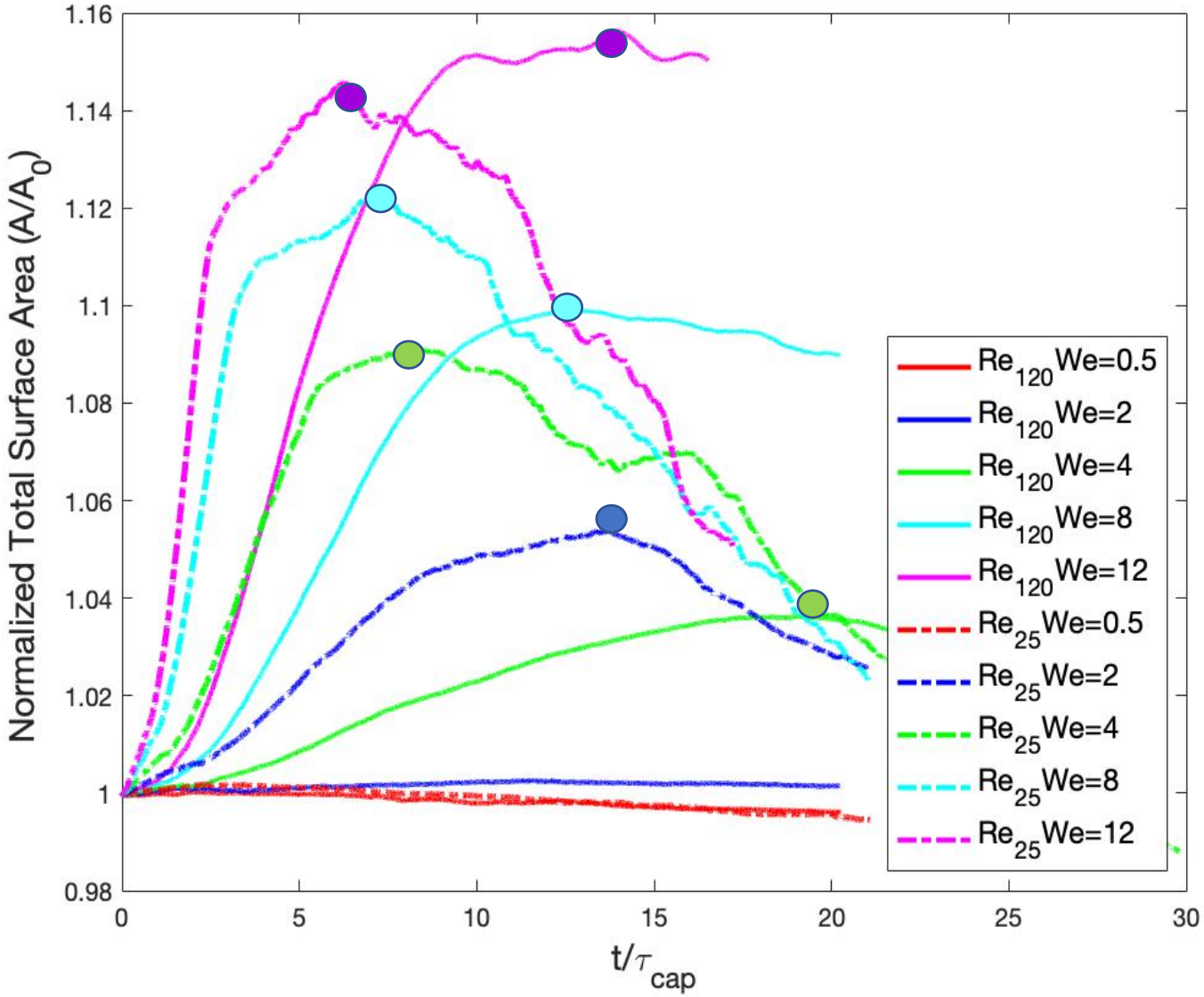

- Initial surface area of the droplet is $A_0 = 4\,\pi\,r^2$.
- At low weber number We =0.5, the normalized surface area doesn't change significantly with change in Reynolds number. This tells that the droplet shape is not changing significantly and stay nearly spherical over the time.
- At a particular Re, as the weber number increases, we observe a peak in normalized area marked with colored circle.
- This suggests that the increase in surface area is one of the contributors in increase in total vaporization rate at all Re and all We.

Study 1: Vaporization flux per unit area $\dot{m}''$ vs time

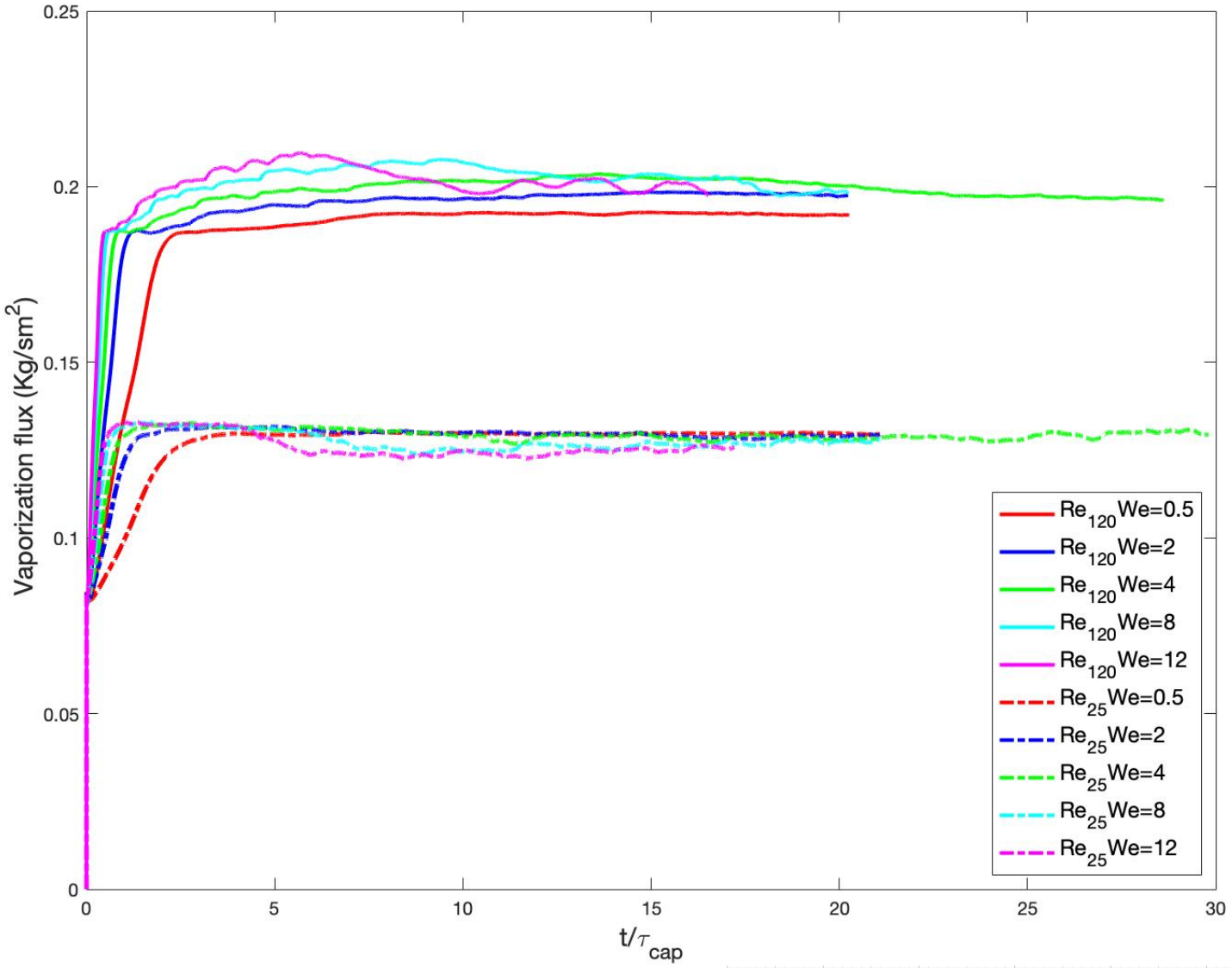

- At a particular Reynolds number, $\dot{m}''$ increases as weber number increases.
- At a particular weber number, $\dot{m}''$ increases with increase in Reynolds number.
- At low Reynolds number (Re=25), the change in $\dot{m}''$ w.r.t. change in weber number is not significant.
- At high Reynolds number (Re=120), the change in $\dot{m}''$ with change in weber number is significant.

Study 1: Vorticity field at different Weber numbers at Re=120

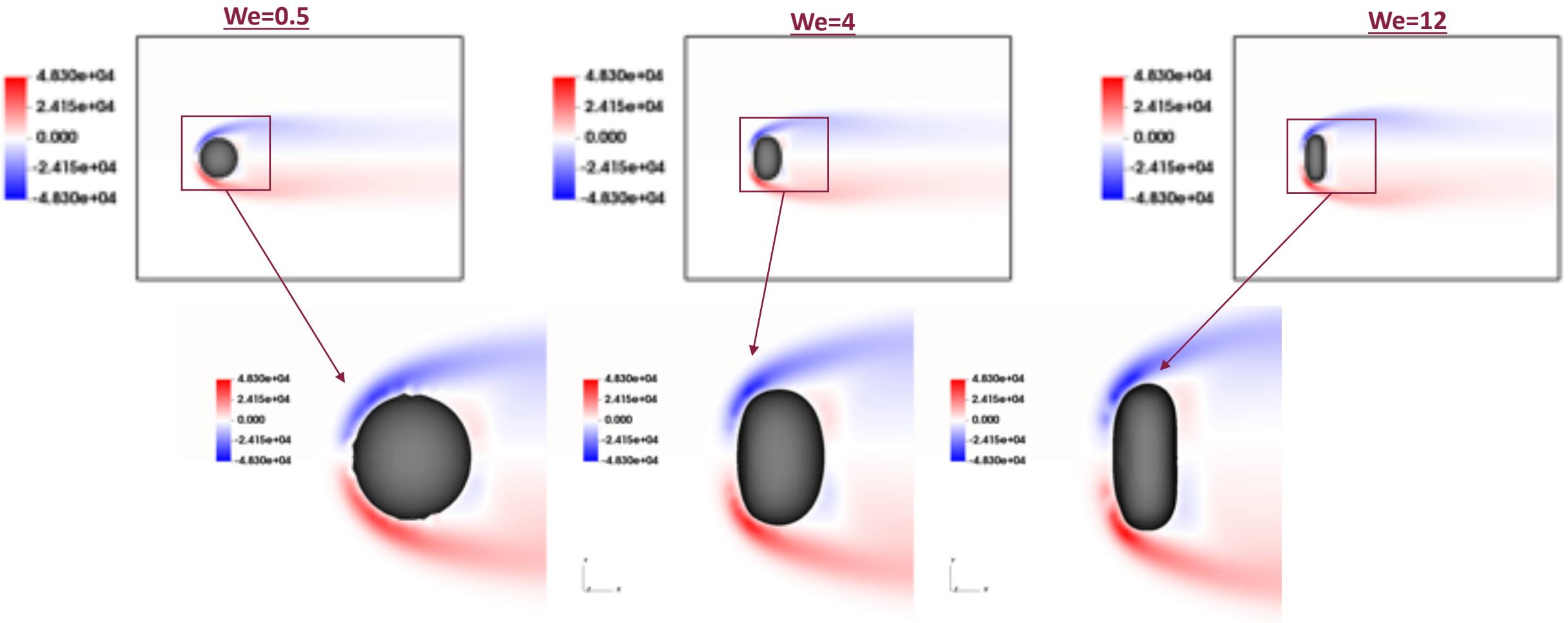

- Vorticity magnitude in z-direction shows clear difference in the rear region of droplet.
- In case of higher weber numbers (We=4,12), the vorticity magnitude is higher behind the droplet.
- Higher deformation of the droplet is leading higher vorticity at the rear which can alter the vaporization rate.

Study 1: $\Delta\ \dot{m}''$ distribution around the droplet at Re=120

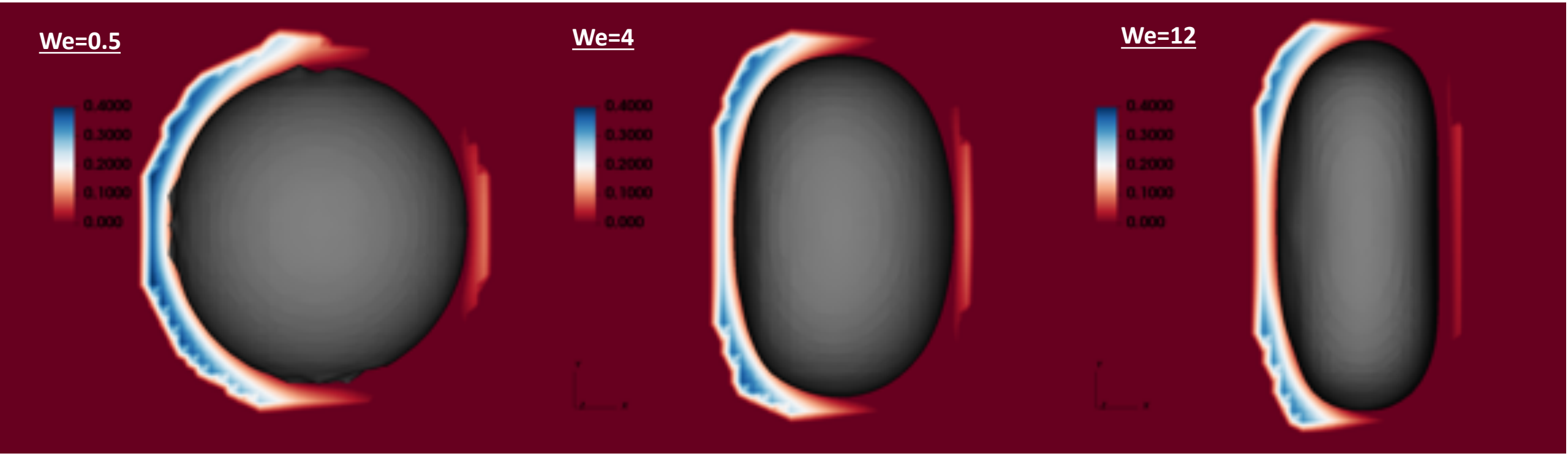

- $\Delta\ \dot{m}'' = \dot{m}''_{local} - \dot{m}''_{average}$, here $\dot{m}''_{average}$ is averaged both space and over time.
- The scale of psuedocolors starts from 0. This means, the plot shows the distribution of vaporization rate per unit area which are higher than $\dot{m}''_{average}$.
- This reveals that most of the vaporization occurs at the front of the droplet.
- Also, additional vaporization is occurring in the rear region as well. This location is same where we observed lower velocity and higher vorticity magnitude.

Study 2: Numerical analysis for different straining flow

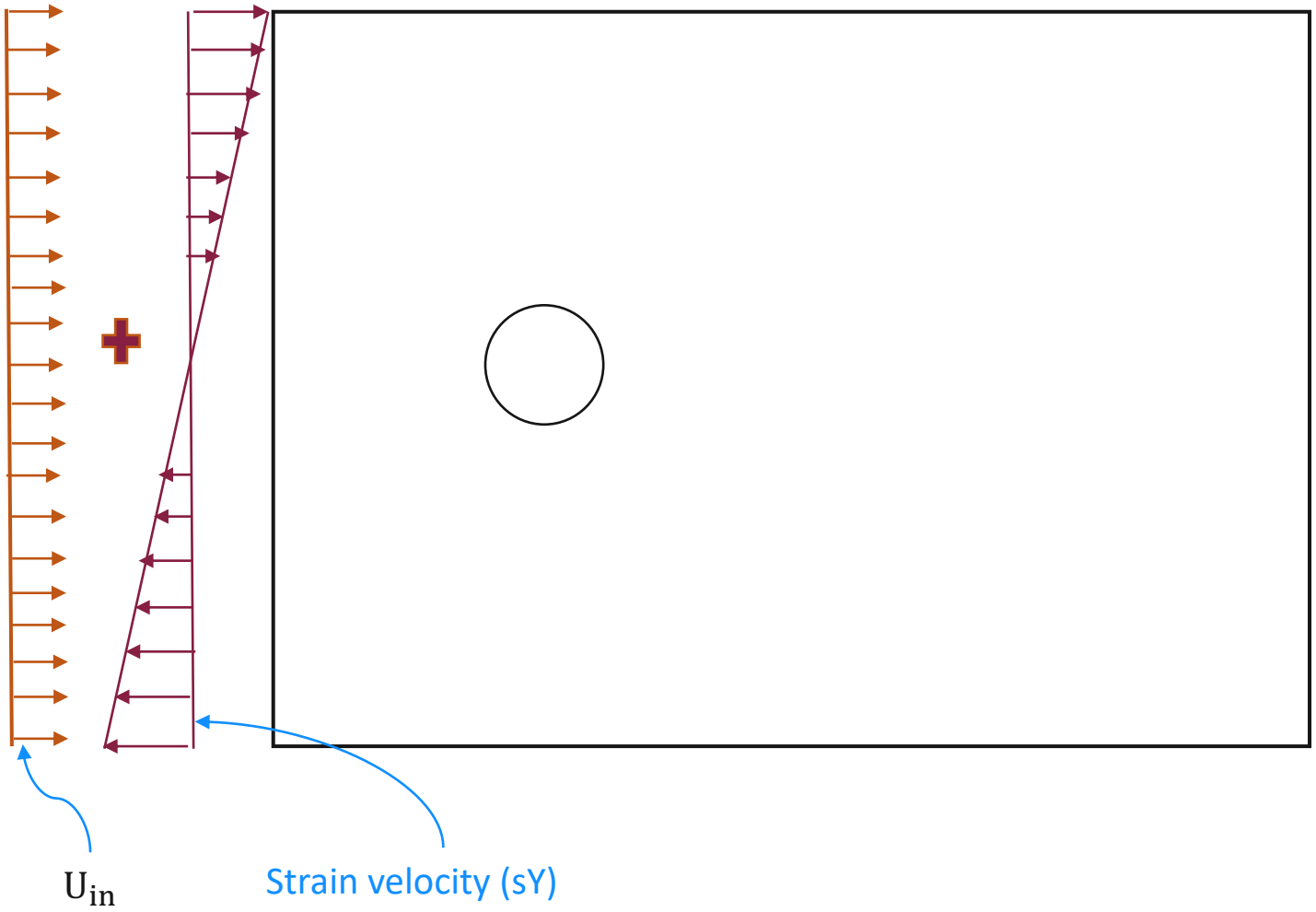

- To understand the effect of straining flow and the droplet shape on vaporization combinedly, we have considered Re=25 with $S_0 = 0$, $S_1 = 0.1U_{in}$, $S_2 = U_{in}$ [2] at We=0.5 and 12.
- This corresponds to $Re_{strain} = \frac{\rho_G S d}{\mu_G} = 0, 2.5 \; and \; 25.$
- In case of straining flow, the inlet velocity varies with Y

$$U = U_{in} + sY$$

here s is strain rate ; s =S /d.

Study 2: Total vaporization rate for different straining flow

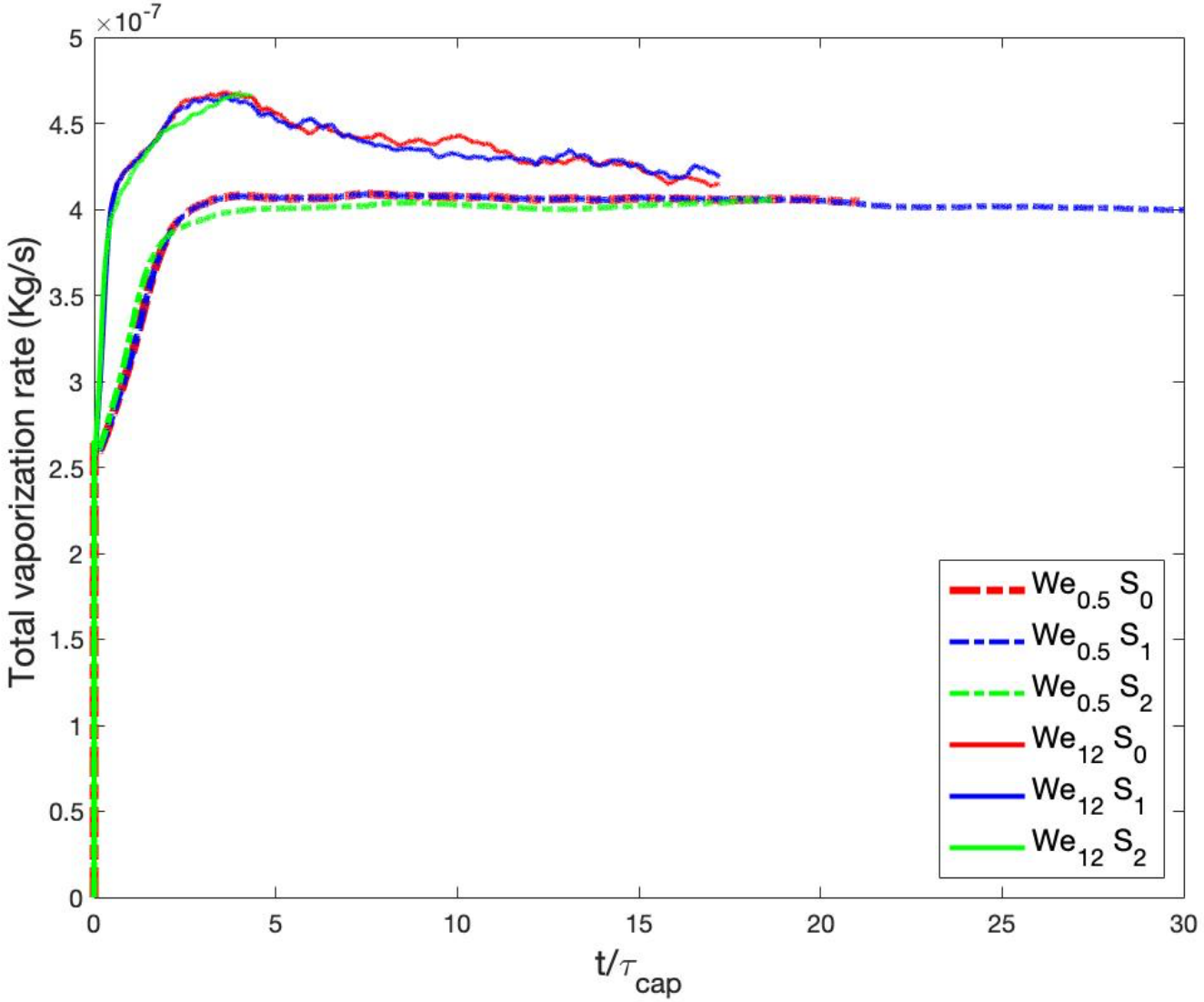

- It is observed that, at low weber number (We=0.5) and low strain case $\mathrm{We}_{0.5}\ \mathrm{S}_1$, the total vaporization rate is closely the same as uniform flow case. However, if the strain rate is increased to $\mathrm{S}_2 = \mathrm{U}_{\mathrm{in}}$, we see change in $\dot{m}$.

- In case of higher weber number We=12, the increase in strain rate show no effect on $\dot{m}$.

.

Study 2: Numerical analysis at different strain rates at We=12, Re=25

Uniform flow

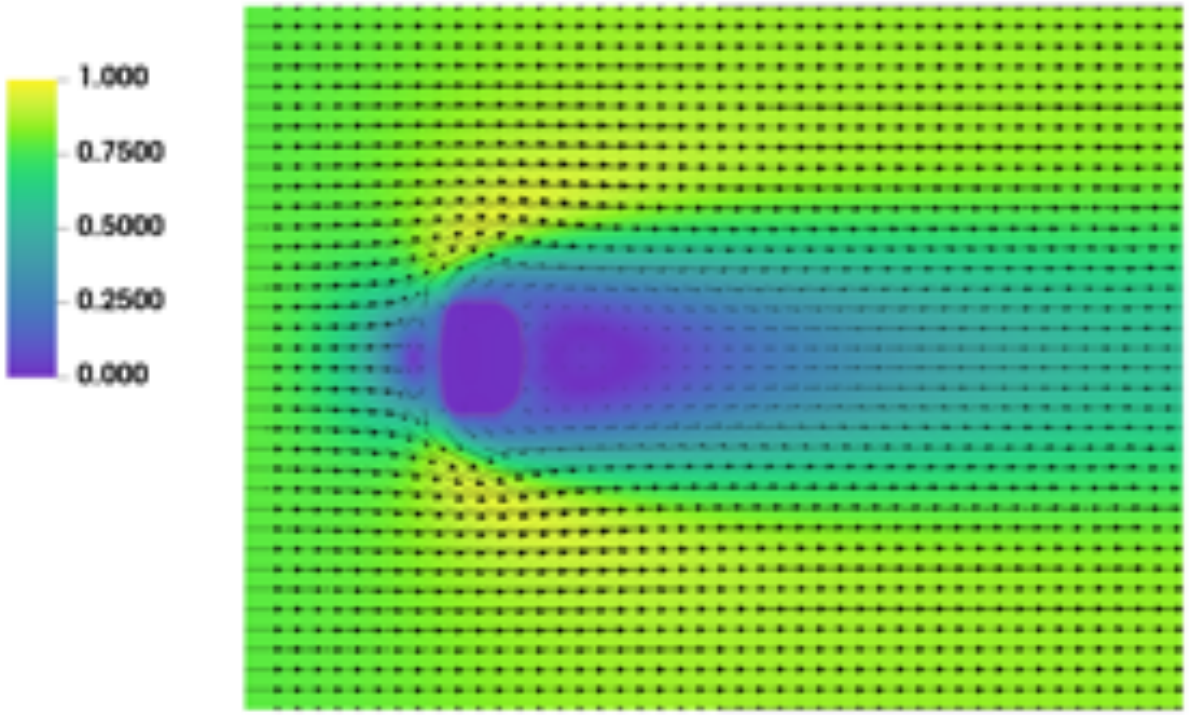

Straining flow $S_2 = U_{in}$

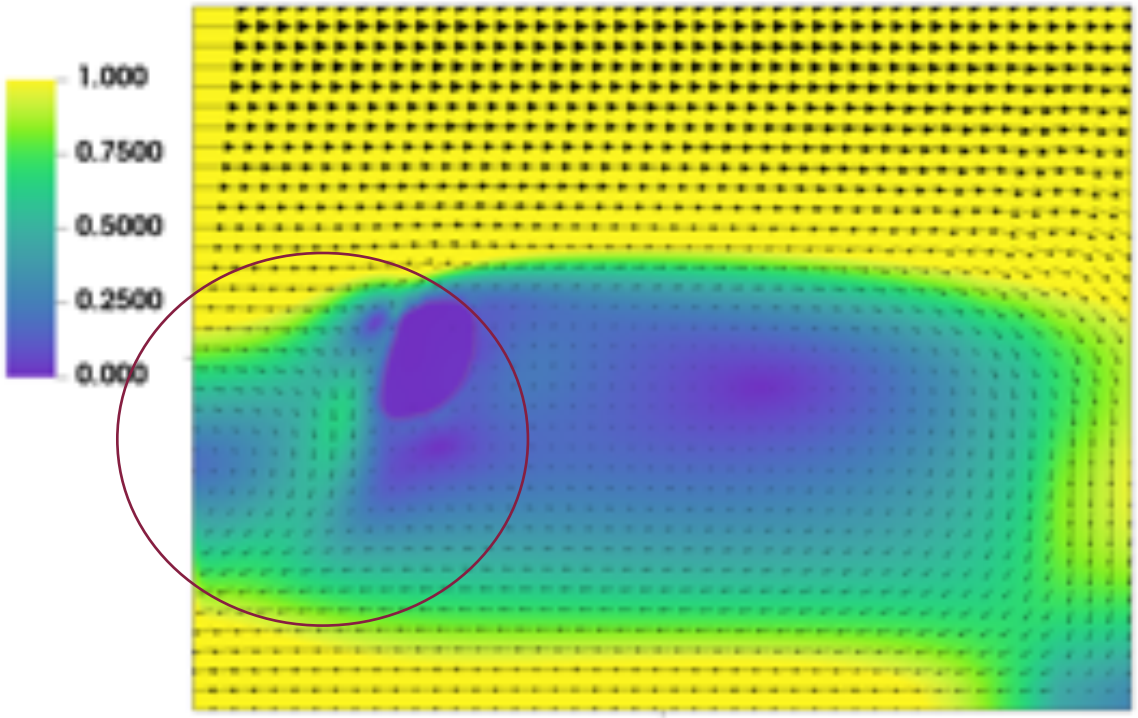

- The visualization of $S_2 = U_{in}$ case show the flow reversal at the inlet as highlighted.

Summary and Future Work

Study 1:

- At a particular Reynolds number, the increase in Weber number leads to increase in deformation of the droplet. This is due to lower surface tension force in the droplet which is available to resist deformation due to inertial forces by ambient fluid.

- For a given Weber number, the vaporization rate increases by increase in Reynolds number .

- For a given Reynolds number, Increase in Weber number show increase in total vaporization rate. This increment is due to both, change in total surface area and local vaporization flux.

- For all flow conditions, local vaporization flux is observed to be located the most in the front of the droplet. Additional vaporization is seen at the rear of the droplet near the wake region at moderate Reynolds number.

Study:2

- In case of non-uniform flow at low Re, we found that lower values of strain velocity do not change the total vaporization rate significantly.

- For the highest strain velocity case in which $\mathrm{Re}_{\mathrm{strain}} = Re_{in}$, we observe that some of the inflow velocity becomes negative which gives erroneous results as shown in previous slide.

Future work:

- Our future work will include the solution of above-mentioned issue and explore the effect of straining flow on vaporization.

Acknowledgement

Thanks to Virginia Tech Advanced Research Computing Center.

Bibliography

1. J. A. Palmore Jr, O. Desjardins, A volume of fluid framework for interface- resolved simulations of vaporizing liquid-gas flows, Journal of Computational Physics 399 (2019) 108954. doi:10.1016/j.jcp.2019.108954.
2. M. Setiya, J. A. Palmore Jr, Method to study effect of straining flow on droplet vaporization at low Reynolds number, in: EasternStates Section of the Combustion Institute, 2020.
3. S. Taneda, Experimental investigation of the wake behind a sphere at low Reynolds numbers, Journal of the Physical Society of Japan 11 (10) (1956) 1104–1108. doi:10.1143/JPSJ.11.1104.
4. E. Achenbach, Vortex shedding from spheres, Journal of Fluid Mechanics 62 (2) (1974) 209–221. doi:10.1017/S0022112074000644.
5. E. Loth, Quasi-steady shape and drag of deformable bubbles and drops, International Journal of Multiphase Flow 34 (6) (2008) 523 – 546. doi: https://doi.org/10.1016/j.ijmultiphaseflow.2007.08.010.
6. An exact solution of the mass transport equations for spheroidal evaporating drops, International Journal of Heat and Mass Transfer 60 (2013) 236 – 240. doi:https://doi.org/10.1016/j.ijheatmasstransfer.2013.01. 001.